Cardiovascular Toxicology
https://doi.org/10.1007/s12012-024-09891-0

RESEARCH

Cardioprotective Effects of 'Vasant Kusumakar Rasa,' a Herbo-metallic Formulation, in Type 2 Diabetic Cardiomyopathy in Rats

Alok D. Singh[1] · **Mukesh B. Chawda**[2] · **Yogesh A. Kulkarni**[1]

Received: 30 March 2024 / Accepted: 1 July 2024

Abstract

Diabetic cardiomyopathy (DCM) is one of the serious complications of type 2 diabetes mellitus. Vasant Kusumakar Rasa (VKR) is a Herbo-metallic formulation reported in Ayurveda, an Indian system of medicine. The present work was designed to study the effect of VKR in cardiomyopathy in type 2 diabetic rats. Diabetes was induced by feeding a high-fat diet (HFD) for 2 weeks followed by streptozotocin (STZ) administration (35 mg/kg *i.p.*). VKR was administered orally at dose of 28 and 56 mg/kg once a day for 16 weeks. The results of the study indicated that VKR treatment significantly improved the glycemic and lipid profile, serum insulin, CK-MB, LDH, and cardiac troponin-I when compared to diabetic control animals. VKR treatment in rats significantly improved the hemodynamic parameters and cardiac tissue levels of TNF-α, IL-1β, and IL- 6 were also reduced. Antioxidant enzymes such as GSH, SOD, and catalase were improved in all treatment groups. Heart sections stained with H & E and Masson's trichome showed decreased damage to histoarchitecture of the myocardium. Expression of PI3K, Akt, and GLUT4 in the myocardium was upregulated after 16 weeks of VKR treatment. The study data suggested the cardioprotective capability of VKR in the management of diabetic cardiomyopathy in rats.

Keywords Vasant Kusumakar Rasa · High-fat diet · Cardiomyopathy · PI3K/Akt/GLUT4 · Oxidative stress · Streptozotocin

Introduction

Type 2 diabetes mellitus (T2DM) is a metabolic disorder that arises due to inappropriate utilization of glucose and progressive loss of β-cell functioning [1]. T2DM impacts the cardiovascular system through a triad of mechanisms: firstly, by inducing coronary artery disease attributed to hastened atherosclerosis; secondly, through the development of cardiac autonomic neuropathy; and lastly, by causing diabetic cardiomyopathy [2]. T2DM leads to various complications and one such life-threatening complication of long-term diabetes is diabetic cardiomyopathy (DCM). It is a particular type of heart disease that is driven by hyperglycemia, insulin resistance, and compensatory hyperinsulinemia. DCM is featured by the presence of structural as well as functional myocardial alterations in the absence of hypertension and coronary artery disease (CAD) that range from early-stage heart failure with diminished systolic function to advanced stage left ventricular hypertrophy and diastolic dysfunction [3]. According to the Framingham research, males with diabetes have a twofold increased risk of developing heart failure, while women with diabetes have a fivefold increased risk [4]. Even with a 32.2% global prevalence of DCM among the type 2 diabetic population, it is treated as an underappreciated disease due to a lack of effective treatment regime [5].

The pathophysiology of DCM initiates from the hyperglycemia-induced impaired cardiac metabolism, microvascular damage, myocardial fibrosis, ventricular hypertrophy, diminished mitochondrial activity, and overactivation of lipid signaling pathway [6]. Individuals with obesity and insulin resistance with type 2 diabetes leads to dyslipidemia,

Handling Editor: Lu Cai.

✉ Yogesh A. Kulkarni
yogeshkulkarni101@yahoo.com

Alok D. Singh
aloksingh463@gmail.com

Mukesh B. Chawda
mbc@solumiks.in

[1] Shobhaben Pratapbhai Patel School of Pharmacy & Technology Management, SVKM's NMIMS, V. L. Mehta Road, Vile Parle (W), Mumbai, Maharashtra 400056, India

[2] Shree Dhootapapeshwar Limited, 135, Nanubhai Desai Road, Khetwadi, Girgaon, Mumbai, Maharashtra 400004, India

Published online: 18 July 2024

causing lipid-induced toxicity in various organs, notably in the cardiac tissue [7]. Circulating advanced glycation end products (AGEs) develop oxidative stress within cells. Impaired glucose metabolism, higher levels of circulating lipids, and fatty deposition activate the systemic inflammatory states resulting in the release of cytokine mediators, such as TNF-α, IL-1β, IL-6, and C-reactive protein (CRP) [8]. To carry out the myocardial contractility, transport of oxygen, substrate for metabolism, and hormones to various regions of the body, the mammalian heart needs a steady supply of glucose as a metabolic fuel to produce ATP. It is believed that fatty acids are the main metabolic substrate for the healthy adult heart [9]. Glucose transporters (GLUTs) are responsible for the transport of glucose through the plasma membrane. GLUT4 serves as the primary mediator of glucose absorption in cardiomyocytes, constituting approximately 70% of the total cardiac GLUTs. Its predominant localization is within intracellular membrane compartments, but upon being stimulated by the hormone insulin, GLUT4 relocates to the cell surface [10]. The impaired insulin metabolic signaling reduces the GLUT4 recruitment to the plasma membrane and affects the glucose uptake, causing a depletion in sarcoplasmic reticulum Ca^{2+} pump activity and raising the intracellular Ca^{2+} levels in cardiomyocytes this contribute to myocardial stiffness in the heart of diabetics [11].

The regulation of glucose and lipid metabolism is governed by the protein AKT. The activation of AKT, which is mainly found in insulin-responsive tissues, facilitates the translation of glucose transporter 4 (GLUT4). An essential component of the insulin signaling cascade is the enzyme phosphatidylinositol 3-kinase (PI3K), which plays a crucial role in mediating the metabolic effects of insulin on glucose transport and the movement of GLUT4. The presence of high blood sugar levels over a prolonged period could directly contribute to the dysfunction of the PI3 kinase/Akt signal pathway. The proper functioning of the PI3K/Akt pathway is necessary for the insulin-dependent regulation of both systemic and cellular metabolism [12, 13]. Previous investigations have provided evidence showcasing the plausible advantageous function of PI3K/Akt-induced GLUT4 relocation in the treatment of DCM [14].

Nowadays, the use of traditional medicine has gained worldwide recognition. A total of one hundred and seventy out of the one hundred and ninety-four Member States of the World Health Organization (WHO) have provided information on the utilization of traditional medicine as a part of the complementary medicine system. Ayurveda is one of the important ancient traditional systems of medicine, originated from India and encompassing a profound understanding of botanical, mineral, and animal-derived remedies. Ayurveda has garnered widespread recognition on a global scale [15]. Vasant Kusumakar Rasa (VKR) is a widely recognized herbo-metallic preparation mentioned in the Ayurveda text, Bharat Bhaishajya Ratnakar and listed in Ayurvedic Formulary of India [16, 17]. VKR is mentioned in the treatment of Prameha, which resembles Diabetes Mellitus and is recognized as an exceptional Rasayana, promoting tissue rejuvenation. VKR is a combination of Suvarna Bhasma (Processed Gold), Rajata Bhasma (Processed Silver), Vanga Bhasma (Processed Tin), Naga Bhasma (Processed Lead), Kantaloha Bhasma (Processed Iron), Abhraka Bhasma (Processed Mica), Pravala Bhasma (Processed Coral), Mouktik Bhasma (Processed Pearl), Rasasindoor (Sublimed red sulfide of Mercury), further treated in Godugdha (Cow milk), Ikshu (*Saccharum officinarum*) Swarasa, Vasa (*Adhatoda vasica*) Swarasa, Shweta (*Santalum album*) Kwath, Usheer (*Vetiveria zizanioides*) Kwath, Rheebera (*Pavonia odorata*) Kwath, Haridra (*Curcuma longa*) Kwath, Kadali (*Musa paradisiaca*) Kwath, Kamal Pushpa (*Nelumbium speciosum*) Swarasa, and Jati Pushpa (*Jasminum officinale*) Swarasa. Earlier research work has established the antihyperglycemic action of VKR and its ability to hinder the advancement and emergence of diabetic retinopathy in an experimental model of Type 1 Diabetes Mellitus [18, 19]. Damage to cardiac tissue serves as a key pathophysiological indicator in the progression of DCM. VKR, known for its tissue rejuvenation properties, may exhibit the capability to enhance the myocardial well-being, consequently slowing down the advancement of DCM. Also to date, no systematic scientific study has been carried out to investigate the efficacy of VKR in delaying or in the management of the DCM. Hence, this study was designed to understand the effect of VKR in high-fat diet and Streptozotocin (STZ)-induced type 2 diabetic cardiomyopathy in rats.

Materials and Methods

Experimental Animals

Male *Sprague Dawley* (SD) rats weighing 180–200 g, 6 to 8 weeks old were procured from the National Institute of Biosciences in Pune, Maharashtra, India. These rodents were accommodated in the institute's animal facility. The designated animal rooms were kept at a controlled temperature of 22 ± 2 °C, a relative humidity of 75 ± 5%, and a 12-h light/dark cycle was maintained. The rats were provided with a fundamental multi-nutritional diet and unrestricted access to purified water ad libitum. The experimental protocol (CPCSEA/IAEC/P-14/2022) was duly approved by the Institutional Animal Ethics Committee. The study was carried out in accordance with the National Institutes of Health (NIH) guide for the care and use of Laboratory animals.

Chemicals and Reagents

Vasant Kusumakar Rasa tablets (Batch no: P220500079) were provided by Shree Dhootapapeshwar Ltd, India. STZ (Lot No.: 022120029) was procured from MP Biomedicals LLC, USA and High-fat diet composed of 60% fat, 20% protein, and 20% carbohydrate (Batch No.: 20-41, Catalogue no. VRKHFD60) was commercially procured from VRK Nutritional Solutions, India. The energy content of HFD was 5200 kcal/kg and its composition comprised of lard, starch, casein, skim milk powder, minerals, and vitamins. Protease cocktail inhibitor and PVDF membrane 0.45 µm (Lot No.: BM2MB0883A) was purchased from Merck, USA. Biochemical kits such as Glucose (Cat # 120200), HbA1c (Cat# 121537), Triglycerides (Cat#120211), Cholesterol (Cat# 120194), LDL-c (Cat# 121261), HDL-c (Cat# 120227) and C-Reactive Protein (CRP) (Cat# 131959), Creatinine Kinase-Myocardial Bundle (CK-MB) (Cat# 120234), and Lactate Dehydrogenase (LDH) (Cat# 120,43) were procured from Transasia Bio-medicals Ltd., India. TGX FastCast Acrylamide kit 10% (Batch No.: 64526770) and Clarity Max Western ECL substrate (Cat #: 1705062) were obtained from Bio-Rad, USA. ELISA kits for Rat insulin (Cat #: KTE101059), Rat Cardiac troponin I (cTn-I) (Cat #: KTE101019), TNF-α (Cat #: KET9007), IL-1β (Cat#: KTE9001), and IL-6 (Cat #: KTE9004) were acquired from Abbkine, USA. The primary antibodies PI3K [20] (sc-1637, Lot #K1622), Akt [21] (sc-5298, Lot # A0623), β-actin [22] (sc-47778, Lot#: I2822), and m-IgG Fc BP-HRP (sc-525409, Lot#: I0622) were bought from Santa Cruz Biotechology Inc, USA. GLUT4 [23] rabbit primary antibody (cat no. 7637) was purchased from Abclonal Technology, USA. All other required chemicals were obtained from Sigma–Aldrich, USA.

Elemental Analysis of VKR

The VKR was characterized using field emission scanning electron microscopy (FESEM)—energy-dispersive spectroscopy (EDS) Quanta 200F, FEI (Netherlands) for the presence of the processed elemental composition.

Experimental Design and Induction of Diabetes

Type 2 diabetes was induced in all rats except normal control by offering HFD for two weeks followed by STZ administration (35 mg/kg, *i.p.*) on the 15th day of the study [24, 25]. Rats with plasma glucose level above 250 mg/dL were confirmed as diabetic and were included in the study by randomly assigning into the various groups. Rats were divided into five groups of six rats ($n = 6$). Group 1 was named as Normal Control and animals received a normal diet and 0.5% carboxymethyl cellulose (CMC) solution for 16 weeks. Group 2 was named as Diabetic Control and animals received HFD throughout the study duration and a single dose of STZ (35 mg/kg, *i.p.*). Group 3 was named as Diabetic + Glipizide (5 mg/kg) and animals were administered orally with Glipizide (5 mg/kg) for 16 weeks. Group 4 was named as Diabetic + VKR (28 mg/kg) and animals were administered with VKR (28 mg/kg, *p.o.*) for 16 weeks. Group 5 was named as Diabetic + VKR (56 mg/kg) and animals were administered with VKR (56 mg/kg, *p.o.*) for 16 weeks. Animals in the group 2, 3, 4, and 5 received HFD throughout the study period. The treatment was given for 16 weeks. At the end of the study, animals were humanely sacrificed using urethane (1.2 g/kg, *s.c.*).

Assessment of Body Weight and Relative Organ Weight

The body weight of the animals from different treatment groups was recorded at the end of the study and the heart weight-to-body weight (HW/BW) ratio was calculated.

Estimation of Biochemical Parameters

Blood was collected from the retro-orbital plexus into an anticoagulant-containing microcentrifuge tube. Subsequently, to separate the plasma, blood samples were subjected to centrifugation at a velocity of 4500 RPM for 20 min. Furthermore, serum was acquired in a microcentrifuge tube devoid of any anticoagulant. The manufacturer's designated protocol was referred to measure glycohemoglobin (HbA1c) in freshly collected whole blood samples. Plasma glucose levels and lipid profile were estimated using commercially available diagnostic kits provided by Transasia Bio-medicals Ltd., India.

Oral Glucose Tolerance Test (OGTT)

After the 16-week treatment period, OGTT was conducted. Before the withdrawal of blood, the animals were subjected to a 6-h fasting period. Subsequently, all subjects received an oral administration of a 40% D-glucose solution in a dosage of 2 g/kg body weight. Blood samples were then taken from the tail vein, and the blood glucose levels were assessed using an ACCU-CHEK glucometer. This evaluation of blood glucose levels occurred at specific intervals of time, namely 0, 30, 60, 90, and 120 min, across all experimental groups [26].

Estimation of Serum Insulin and Homeostatic Model Assessment for Insulin Resistance (HOMA-IR)

Insulin level in serum sample was determined using a rat insulin enzyme-linked

immunosorbent assay (ELISA) kit (Abbkine, USA). Homeostatic Model Assessment for Insulin Resistance (HOMA-IR) was calculated using the formula [27]:

$$\text{HOMA} - \text{IR} = (\text{fasting insulin} \times \text{fasting glucose})/22.5$$

Recording of Hemodynamic Parameters

The surgical procedure was carried out by giving an incision on the center of the chest. The rats were anesthetized with *ip* injection of urethane (1.2 g/kg). The left carotid artery was cannulated and a polyethylene catheter PE10 was connected to a pressure transducer attached to the Power lab Data acquisition system, (AD instrument, Australia). The cannulated animal was kept for 10 min to stabilize and then heart rate, systolic blood pressure (SBP), diastolic blood pressure (DBP), mean atrial pressure (MAP), PR interval, QRS interval, and maximum and minimum rate of ventricular contraction (+dp/dt, − dp/dt) were recorded. Simultaneously, three electrodes (+ ve, −ve, and neutral) were attached to the rats to record the changes in ECG [28].

Estimation of the Cardiac Injury Markers

Serum levels of Creatinine kinase-myocardial bundle (CK-MB) and Lactate dehydrogenase (LDH) were estimated using diagnostic kits provided by Transasia Bio-medicals Ltd. India. Serum cardiac troponin-I (cTn-I) was estimated using ELISA kits supplied by Abbkine, USA.

Estimation of Inflammatory Markers

C-Reactive protein (CRP) was estimated in the serum sample using diagnostic kits supplied by Transasia Bio-medicals Ltd. India. TNF- α, IL-1β, and IL-6 were estimated in cardiac tissue homogenate. Insulin concentration was measured using rat ELISA kits supplied by Abbkine, USA.

Determination of Oxidative Stress Parameters

A 10% (w/v) cardiac tissue homogenate was prepared for the evaluation of oxidative stress parameters using a homogenizer from Kinematica, Switzerland. The homogenate was prepared in a phosphate buffer with a pH value of 7.4 and a concentration of 50 mM. Within the cardiac tissue homogenate, the levels of malondialdehyde (MDA) [29], superoxide dismutase (SOD) [30], catalase (CAT) [31], and reduced glutathione (GSH) [32] were determined.

Histopathology Analysis

At the end of the study, animals were sacrificed using urethane (1.2 g/kg, *s.c.*) as terminal anesthesia. Cardiac tissue was isolated and fixed in 10% buffered formalin. Formalin-fixed tissues of cardiac tissue were trimmed and subjected to tissue processing using different grades of alcohol followed by xylene cleaning. The tissue was further embedded using paraffin wax. Paraffin wax-embedded tissue blocks were sectioned using a rotary microtome. Slides of cardiac tissue were stained with Hematoxylin and Eosin (H & E) stain and Masson's Trichome stain. The visualization of stained slides was done using a photographic microscope from Motic, Canada.

Western Blot Analysis

Myocardial tissue was homogenized with radioimmunoprecipitation assay (RIPA) lysis buffer, and the protein concentration was determined. In brief, the cardiac tissue protein was separated using Biorad's sodium dodecyl sulfate–polyacrylamide gel electrophoresis (SDS–PAGE) and subsequently transferred onto a nitrocellulose membrane, which was then blocked for 2 h using 5% non-fat dry milk. Subsequently, the membrane was incubated overnight at 4◦C with a rat primary antibody. The resulting blots were subjected to Chemi-Doc XRS visualization unit (Bio-Rad, USA) to measure the expression levels of PI3K, Akt, GLUT4, and β-actin and were quantified using ImageJ software, NIH, USA.

Statistical Analysis

The data are expressed as mean ± SEM. The statistical significance was analyzed by ANOVA followed by Dunnett's post hoc test using a graphpad prism version 8.4.2 software, USA. The value of $p < 0.05$ was considered statistically significant.

Results

Elemental Analysis of VKR

VKR exhibited the presence of various elements, namely magnesium (Mg), silicon (Si), phosphorus (P), calcium (Ca), iron (Fe), calcium (Ca), tin (Sn), oxygen (O), carbon (C), silver (Ag), gold (Au), mercury (Hg), and lead (Pb) (Fig. 1; Table 1). All the metallic elements mentioned in the formulation of VKR were detected.

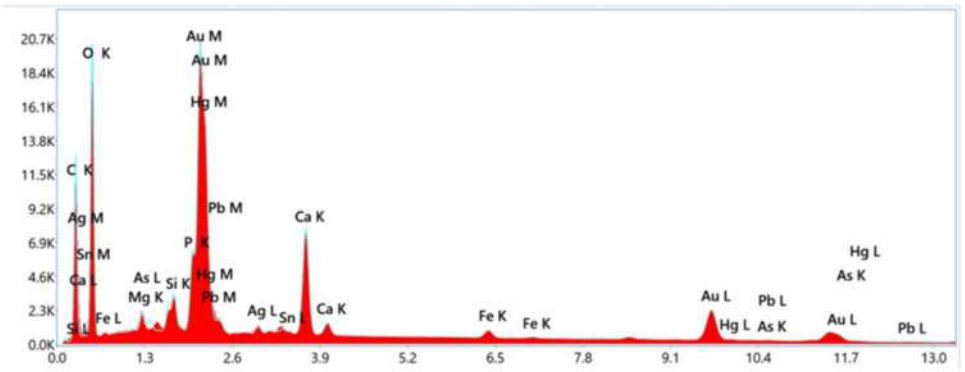

Fig. 1 Elemental analysis of VKR

Table 1 Elemental composition of VKR

Sr. No	Element	Weight (%)	Atomic (%)
1	C K	31.1	55.0
2	O K	27.7	36.8
3	Mg K	0.2	0.2
4	Si K	0.6	0.5
5	P K	1.6	1.1
6	Ca K	4.8	2.6
7	Fe K	0.7	0.3
8	As K	0.0	0.0
9	Ag L	0.6	0.1
10	Sn L	0.3	0.0
11	Au L	30.8	3.3
12	Hg L	0.9	0.1
13	Pb L	0.8	0.1

Effect of VKR Treatment on Body Weight and Relative Organ Weight

The animals in the diabetic control group showed a significant ($p < 0.001$) increase in body weight in comparison to the animals in the normal control group. In contrast, the body weight of all the treatment groups exhibited a significant ($p < 0.001$) decrease when compared to the animals in the diabetic control group (Fig. 2). The HFD-STZ diabetic group exhibited a significant ($p < 0.001$) increase in the ratio of heart weight to body weight when compared to the control. On the other hand, the VKR-treated diabetic groups demonstrated a significant ($p < 0.01$, $p < 0.001$) decrease in the ratio of heart weight to body weight when compared to the diabetic control group (Fig. 2).

Effect of VKR Treatment on Glycemic Profile

Animals in the diabetic control group illustrated a significant ($p < 0.001$) increase in plasma glucose levels, HbA1c levels, insulin levels, and HOMA-IR assessment compared to the normal control group animals. The animals in all the treatment groups displayed a significant ($p < 0.001$) decrease in the elevated levels of the glycaemic profile, viz., plasma glucose HbA1c, insulin, and HOMA-IR compared to the animals in the diabetic control group (Fig. 3). Furthermore, the results of the glycemic profile with VKR treatment were comparable to the glipizide-treated group. In the case of OGTT, the plasma glucose levels at 30, 60, 90, and 120 min exhibited a significant ($p < 0.001$) increase in the diabetic control group when compared to the normal control group. In all treated groups, the plasma glucose levels at 30, 60, 90, and 120 min demonstrated a notable ($p < 0.001$) decrease in comparison to the diabetic control group (Fig. 3).

Fig. 2 Effect of VKR treatment on body weight and relative organ weight. All values are expressed as mean ± SEM ($n = 6$). $^{###}p < 0.001$ when the diabetic control group compared with normal control group. $^{***}p < 0.001$, $^{**}p < 0.01$, $^{*}p < 0.05$ when treatment group compared with diabetic control group

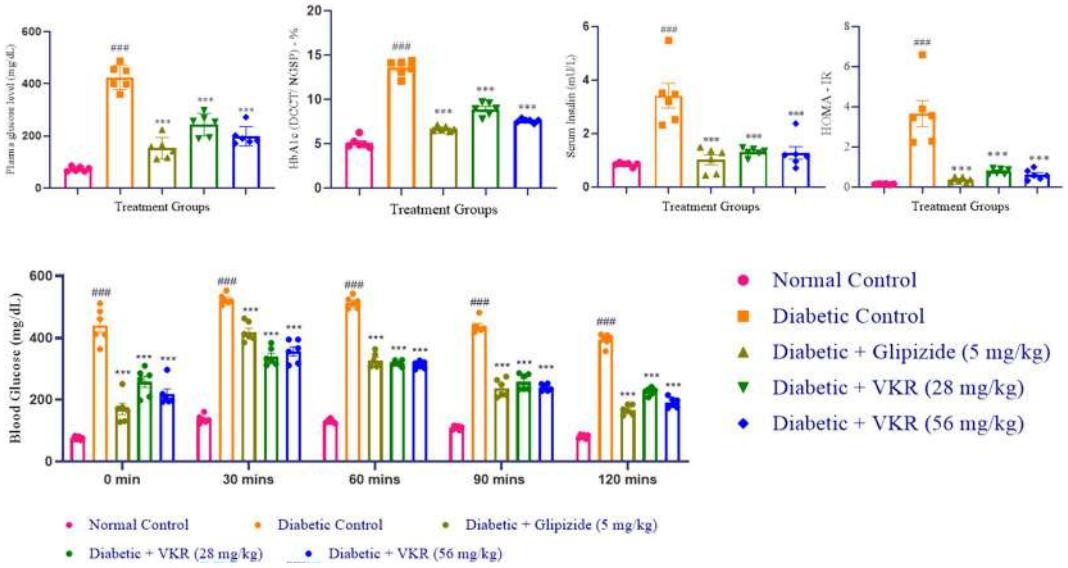

Fig. 3 Effect of VKR treatment on glycemic profile. All values are expressed as mean ± SEM ($n = 6$). $^{###}p < 0.001$ when the diabetic control group compared with normal control group. $^{***}p < 0.001$ when treatment groups compared with the diabetic control group

Effect of VKR Treatment on Lipid Parameters

The animals in the diabetic control group showed a significant ($p < 0.001$) increase in lipid parameters such as triglycerides, cholesterol, and LDL in comparison to the animals in the normal control group. All the treatment groups exhibited a significant ($p < 0.001$) decrease in the mentioned lipid parameters when compared to the animals in the diabetic control group (Table 2). The HFD-STZ diabetic control group exhibited a significant ($p < 0.001$) decrease in the HDL level when compared to the normal control group. VKR-treated diabetic animals demonstrated a significant, ($p < 0.01$, $p < 0.001$) increase in HDL level when compared to the diabetic control group.

Effect of VKR Treatment on Hemodynamic Assessment

As depicted in (Fig. 4), rats with diabetes exhibited a significant ($p < 0.001$) decrease in heart rate, SBP, DBP, and MAP in comparison to the rats in the normal control group; however, the administration of glipizide (5 mg/kg), VKR at 28, and 56 mg/kg significantly ($p < 0.001$) increased heart rate, SBP, DBP, and MAP in the rats. In addition, diabetic rats demonstrated a significantly ($p < 0.001$) prolonged PR interval and significant ($p < 0.001$) delay of QRS interval when compared to the normal rats. All the treatment groups exhibited a significant ($p < 0.001$) shortening of PR interval and significant ($p < 0.001$) change in QRS interval when compared to animals in the diabetic control group. As illustrated in Fig. 4, diabetic rats displayed a significant ($p < 0.001$) decrease in the maximum rate of ventricular activity (+ dp/dt) and significant increase in the minimum rate of ventricular activity (–dp/dt) in diabetic control animals when compared with normal control animals. Treatment with VKR at doses 28 and 56 mg/kg significantly ($p < 0.001$) increased + dp/dt and significantly ($p < 0.001$) affected –dp/dt.

Table 2 Effect of VKR treatment on lipid profile

Parameters	Normal control	Diabetic control	Diabetic + glipizide (5 mg/kg)	Diabetic + VKR (28 mg/kg)	Diabetic + VKR (56 mg/kg)
Triglycerides (mg/dL)	52.17 ± 7.58	310.2 ± 13.31$^{###}$	190.3 ± 15.66***	197.8 ± 11.11***	184.0 ± 11.61***
Cholesterol (mg/dL)	64.33 ± 6.99	224.5 ± 18.54$^{###}$	126.7 ± 2.90***	148.8 ± 5.65***	130.3 ± 8.028***
HDL-c (mg/dL)	47.50 ± 1.83	18.67 ± 1.47$^{###}$	35.17 ± 2.79***	30.67 ± 2.27**	38.83 ± 2.18***
LDL-c (mg/dL)	18.33 ± 2.67	70.00 ± 3.23$^{###}$	34.676 ± 2.02***	41.67 ± 3.13***	31.50 ± 1.97***

All values are expressed as mean ± SEM ($n = 6$). $^{###}p < 0.001$ when the diabetic control group compared with the normal control group. $^{***}p < 0.001$, $^{**}p < 0.01$ when treatment groups compared with the diabetic control group

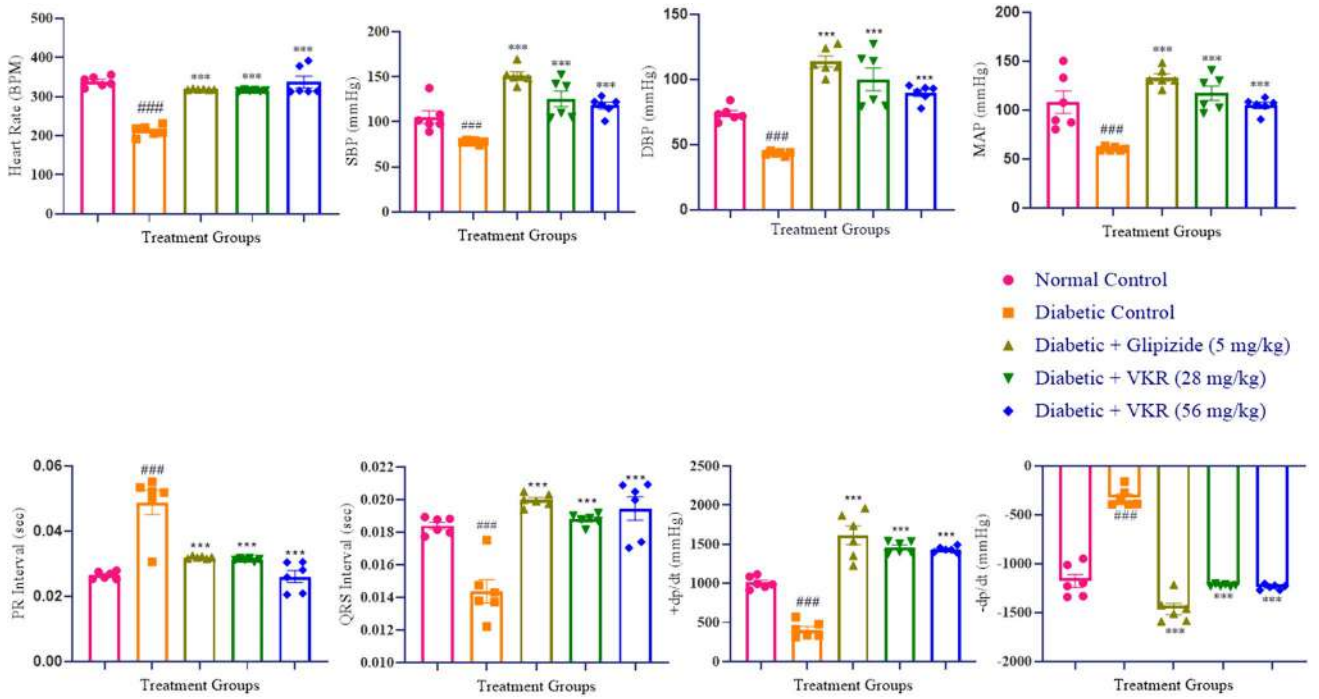

Fig. 4 Effect of VKR treatment on hemodynamic assessment. All values are expressed as mean ± SEM ($n = 6$). $^{###}p < 0.001$ when the diabetic control group compared with the normal control group. $^{***}p < 0.001$ when treatment groups compared with the diabetic control group

Effect of VKR Treatment on Cardiac Injury and Pro-Inflammatory Biomarkers

Animals in the diabetic control group showed significantly ($p < 0.001$) elevated levels of CK- MB, LDH, and cTn-I levels when compared to animals in the normal control group. Treatment with VKR at both dose levels for 16 weeks significantly ($p < 0.001$) reduced the elevated levels of the cardiac injury biomarkers, viz., CK-MB, LDH, and cTn-I when compared to animals in the diabetic control group. Additionally, pro-inflammatory markers such as serum CRP and TNF-α, IL-1β, and IL-6 in cardiac tissue were significantly ($p < 0.001$) increased in the diabetic control group. Treatment with VKR (28 mg/kg and 56 mg/kg) significantly ($p < 0.001$) reduced the serum CRP levels and cardiac tissue levels of IL-1β and IL-6 when compared to animals in the diabetic control group. TNF-α levels in VKR-treated groups were significantly ($p < 0.05$) reduced when compared to animals in diabetic control group. Also, treatment with Glipizide (5 mg/kg) significantly reduced the elevated levels of cardiac injury and pro-inflammatory markers when compared to animals in the diabetic control group (Table 3).

Effect of VKR Treatment on Cardiac Oxidative Stress Parameters

Animals in the diabetic control group demonstrated a significant ($p < 0.001$) increase in MDA levels and a significant ($p < 0.001$) decrease in GSH, CAT, and SOD levels when compared to the normal control group animals. In contrast, the groups treated with VKR (28 mg/kg), VKR (56 mg/kg), and Glipizide (5 mg/kg) for 16 weeks showed a significant ($p < 0.001$) reduction in elevated MDA levels compared to the animals in the diabetic control group. Similarly, these treatment groups exhibited a significant ($p < 0.001$) restoration in reduced GSH levels compared to the diabetic control group. Additionally, the groups treated with Glipizide (5 mg/kg) and VKR (56 mg/kg) demonstrated a significant ($p < 0.01$, $p < 0.05$) increase in reduced CAT levels compared to the animals in the disease control group. However, the treatment with VKR (28 mg/kg), VKR (56 mg/kg), and Glipizide (5 mg/kg) significantly ($p < 0.01$, $p < 0.001$. $p < 0.05$) increased the SOD levels in the all the treatment groups (Table 4).

Table 3 Effect of VKR Treatment on cardiac injury and pro-inflammatory biomarkers

Parameters	Normal control	Diabetic control	Diabetic + glipizide (5 mg/kg)	Diabetic + VKR (28 mg/kg)	Diabetic + VKR (56 mg/kg)
CK-MB (IU/L)	636.5 ± 26.41	1605 ± 89.43$^{###}$	849.2 ± 40.64***	898.3 ± 40.64***	787.5 ± 49.31***
LDH (IU/L)	161.5 ± 6.02	368.0 ± 21.27$^{###}$	253.2 ± 13.38***	238.3 ± 9.82***	220.7 ± 4.91***
cTn-I (ng/ml)	10.98 ± 1.08	47.51 ± 8.41$^{###}$	23.15 ± 3.31**	18.44 ± 1.87***	14.02 ± 1.84***
CRP (mg/dL)	0.73 ± 0.04	1.50 ± 0.05$^{###}$	1.16 ± 0.03***	1.15 ± 0.03***	1.12 ± 0.03***
TNF-α (pg/ml)	180.7 ± 17.87	839.6 ± 120.3$^{###}$	437.1 ± 127.3*	434.8 ± 96.91*	399.0 ± 87.73*
IL-1β (pg/ml)	700 ± 83.34	3537 ± 338.2$^{###}$	1752.0 ± 357.2***	1573.0 ± 167.9***	1437.0 ± 216.1***
IL-6 (pg/ml)	903.8 ± 154.9	5923.0 ± 459.9$^{###}$	2386.0 ± 178.9***	1507.0 ± 348.9***	1259.0 ± 47.39***

All values are expressed as mean ± SEM ($n = 6$). $^{###}p < 0.001$ when the diabetic control group compared with the normal control group. ***$p < 0.001$, **$p < 0.01$, and *$p < 0.05$ when treatment groups compared with the diabetic control group

Table 4 Effect of VKR treatment on cardiac oxidative stress parameters

Parameters	Normal control	Diabetic control	Diabetic + glipizide (5 mg/kg)	Diabetic + VKR (28 mg/kg)	Diabetic + VKR (56 mg/kg)
MDA (μMol/mg of protein)	1.40 ± 0.10	7.94 ± 0.51$^{###}$	5.46 ± 0.33***	3.20 ± 0.41***	2.13 ± 0.20***
CAT (μm of H_2O_2 decomposed/min/mg of protein)	0.41 ± 0.02	0.12 ± 0.01$^{###}$	0.38 ± 0.06**	0.26 ± 0.03	0.35 ± 0.06*
SOD (U/mg of protein)	0.60 ± 0.02	0.18 ± 0.004$^{###}$	0.33 ± 0.03*	0.37 ± 0.04**	0.48 ± 0.03***
GSH (μMol/mg of protein)	23.95 ± 0.87	4.75 ± 0.44$^{###}$	11.33 ± 0.71***	11.58 ± 1.17***	15.44 ± 1.14***

All values are expressed as mean ± SEM ($n = 6$). $^{###}p < 0.001$ when the diabetic control group compared with the normal control group. ***$p < 0.001$, **$p < 0.01$, and *$p < 0.05$ when treatment groups compared with the diabetic control group

Effect of VKR Treatment on Myocardial Histology (H & E stain)

The cardiac tissue of animals with diabetes exhibited a range of lesions, including multifocal moderate lymphocytic infiltration and mild degeneration. In contrast, normal control animals displayed less lymphocytic infiltration or degeneration (Fig. 5).

Effect of VKR Treatment on Myocardial Histology (Masson's Trichome Stain)

Cardiac tissue of normal control animals did not show deposition of collagen in the myocardium. Diabetic control animals showed multifocal deposition of collagen in the myocardium. Treatment with VKR at both doses showed notably reduced collagen deposition in cardiac tissue (Fig. 6).

Effect of VKR Treatment on PI3K/Akt/GLUT4

In Western blot analysis, a significant decrease in the expression of PI3K, Akt, and GLUT4 ($p < 0.001$) was observed in the diabetic control group as compared to normal control group. VKR treatment (28 mg/kg and 56 mg/kg) for 16 weeks significantly ($p < 0.001$) increased the expression of PI3K protein when compared to diabetic control animals. Akt levels were significantly ($p < 0.05$) increased in Glipizide (5 mg/kg) and VKR (56 mg/kg) when compared to animals in the diabetic control group. Rats in VKR (28 mg/kg) and Glipizide (5 mg/kg) treated groups showed significant ($p < 0.05$) increase in expression of GLUT4 as compared to rats in the diabetic control group. VKR at a dose of 56 mg/kg showed a significant ($p < 0.01$) increase in the expression of GLUT4 (Fig. 7).

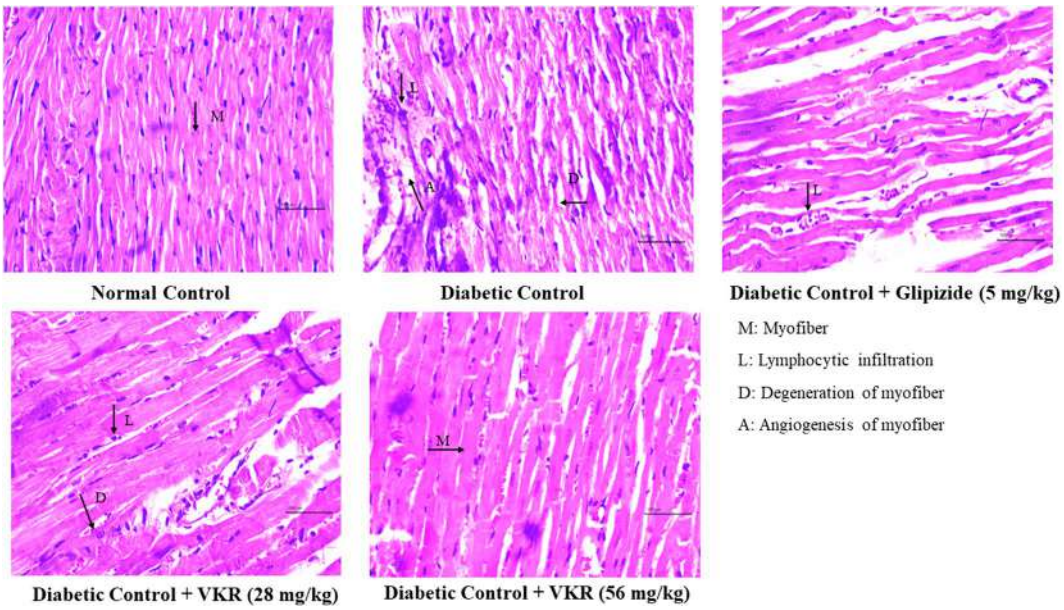

Fig. 5 Effect of VKR treatment on myocardial histology (H & E stain). Normal control showing normal histology of myofibers (M). Diabetic control shows lymphocytic infiltration (L) and degeneration of myofibers (D). Glipizide (5 mg/kg)-treated animals showed normal histology of myocardium. VKR (28 mg/kg) showing mild lymphocytic infiltration (L) and degeneration of myofibers (D). VKR (56 mg/kg) normal histology of myofibers (M)

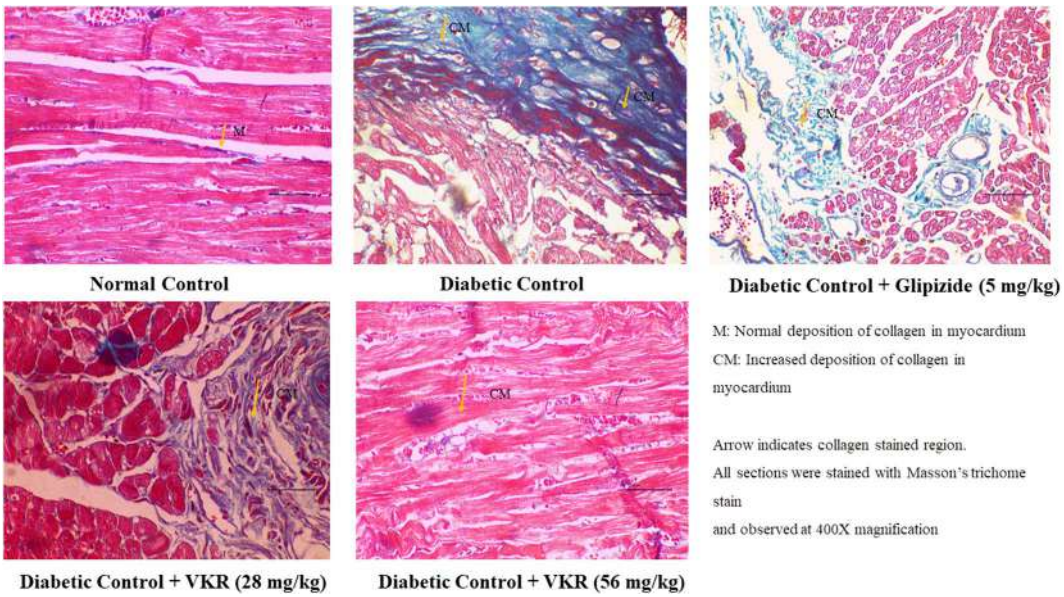

Fig. 6 Effect of VKR treatment on myocardial histology (Masson's Trichome stain). Normal control showed normal collagen deposition in cardiac tissue (M). Diabetic control showed increased deposition of collagen (CM). Glipizide (5 mg/kg) treated animals showed moderate deposition of collagen (CM). VKR (28 mg/kg) showed a lower deposition of collagen (CM). VKR (56 mg/kg) showed a normal deposition of collagen (CM)

Discussion

Over centuries, traditional medicines have been recognized as an additional and alternative medical system. It is important to remember, nevertheless, that very few medications and formulations made from traditional systems have been evaluated by science. Thus, to provide a solid scientific basis for these traditionally derived medications, it is essential to keep generating scientific evidence. One

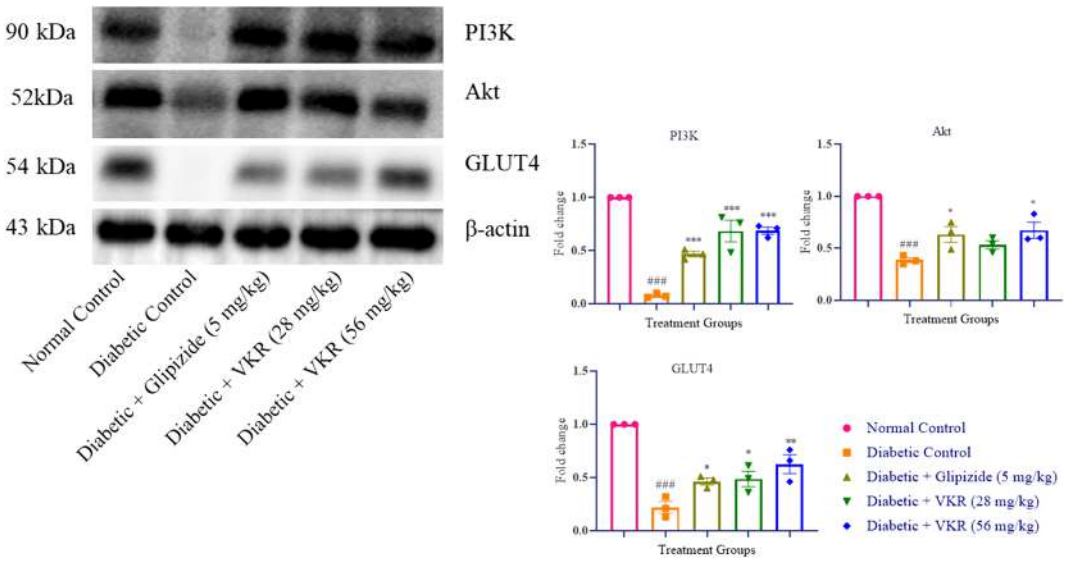

Fig. 7 Effect of VKR treatment on PI3K/Akt/GLUT4 pathway. All values are expressed as mean ± SEM ($n = 3$). $^{###}p < 0.001$ when diabetic control group compared with normal control group. $***p < 0.001$, $**p < 0.01$, $*p < 0.05$ when treatment groups compared with diabetic control group. The original blots are presented in the supplementary file (Fig. 8 & 8A, Fig. 9 & 9A, Fig. 10 & 10A, Fig. 11 & 11A, respectively)

such Ayurvedic herbo-metallic compound that has been widely used in clinical practice to treat diabetes is VKR. No scientific research has been done to assess its effectiveness despite its extensive usage. Thus, the primary objective of this study was to evaluate the effect of VKR in the treatment of DCM using continuous high-fat diet (HFD) and STZ in SD rats. The study results reported presence of cardiac dysfunction sourced by hyperglycemia, hyperinsulinemia, and insulin resistance. The study ultimately observed a well-regulated glycemic profile, which could potentially be attributed to the efficient utilization of glucose. This was further supported by the notable reduction in glycohemoglobin and serum insulin levels. Additionally, the treatment groups demonstrated proficient improvement in glucose homeostasis, thus establishing VKR as a promising antidiabetic candidate.

Studies have demonstrated the direct influence of the consumption of a diet rich in calories and STZ on the weight of the body [33]. In current study protocol, lard-rich high-fat diet served as a major source of energy for the experimental animals. The study model employed in the present work increased the body weight, signifying the development of obesity, through continuous feeding of the high-fat diet and partial destruction of β pancreatic cells by STZ. A decrease in body weight was observed across the treatment group, indicating that VKR possesses the capability to effectively utilize body fat, thereby resulting in a reduction in body weight.

Cardiac hypertrophy serves as a robust indicator for cardiovascular events and is frequently observed in individuals with diabetic myocardium. The administration of VKR at both dosage levels effectively reduced the heart weight by body weight ratio, thereby indicating a decrease in the hypertrophy of cardiac tissue following a 16-week treatment. The decline in myocardial hypertrophy may be attributed to VKR's ability to mitigate the alterations in cellular functioning caused by diabetes, which in turn affects the anabolic insulin signaling responsible for the myocardial wall thickness and enlargement of the left ventricular cavity or both. It is worth noting that other molecular and metabolic mechanisms may also contribute to this condition in a synergistic and potentially independent manner [34].

Oxidation of fatty acids generates a higher amount of ATP per molecule in comparison to glucose. Consequently, it is not surprising that tissues with high energy demands, such as cardiomyocytes, predominantly rely on circulating lipids for energy, making them one of the primary sites for fatty acid uptake. Prolonged dysregulation between the uptake and oxidation of fatty acids can lead to the accumulation of cellular lipids within the myocardium, which can have negative effects on cardiomyocyte metabolism and functionality [35, 36]. The study demonstrated that there was a notable elevation in circulating lipid levels in diabetic rats, and the administration of VKR for a duration of 16 weeks resulted in a significant decrease in lipid accumulation. Furthermore, the VKR treatment exhibited a significant improvement in plasma cholesterol, triglycerides, HDL-c, and LDL-c levels when compared to the diabetic control animals.

The serum concentrations of CK-MB, LDH, and cTn-I are pivotal cardiac markers and are crucial indicators of myocardial injury [37, 38]. These enzymes are released into the bloodstream when the myocardium is metabolically impaired due to hyperglycemia. In the diabetic control rats, the serum concentrations of CK-MB, LDH, and cTn-I were significantly elevated compared to the control group rats, indicating noteworthy damage to the myocardium. However, after 16 weeks of VKR treatment, the myocardial damage was significantly ameliorated as evidenced by a reduction in the serum levels of CK-MB, LDH, and cTn-I representing its cardioprotective effect. The findings of this study are in line with the previous research [39].

Hyperglycemia serves as a crucial prerequisite for the initiation of multiple chemokines, cytokines, and leukocyte adhesion molecules, which subsequently lead to the occurrence of myocardial inflammation [40]. The process of myocardial inflammation is characterized by its heterogeneous nature, involving multiple pathways that are fuelled by chronic low-grade inflammation that initiates the structural and metabolic alterations in the myocardium of individuals with diabetes, leading to cardiac fibrosis and disturbances in myocardial calcium handling [41]. Consequently, these changes contribute to the development of diabetic cardiomyopathy. Study reports from earlier studies support the information that pro-inflammatory cytokines, namely IL-6, IL-1β, and TNF-α, play a pivotal role in the pathogenesis of diabetic cardiomyopathy [42]. In the present study, a significant rise in the levels of pro-inflammatory cytokines was observed in rats with type 2 diabetes mellitus. However, the administration of VKR resulted in a noteworthy reduction in the concentrations of IL-6, IL-1β, and TNF-α in the cardiac tissues of diabetic rats.

The manifestation of cardiac abnormalities resulting from an abundance of glucose in the bloodstream is readily evident in the electrocardiogram (ECG). Decrease in heart rate, abnormal arterial pressure, and changes in the QRS interval, which signifies a delay in ventricular depolarization are the signs of cardiac dysfunction. Prolongation of the PR interval indicates delayed conduction of the sinoatrial node and is associated with an increased risk of atrial fibrillation [25, 43]. The diabetic animals showed a statistically significant increase in the PR interval and a significant decrease in heart rate, arterial pressure (systolic blood pressure, diastolic blood pressure, and mean arterial pressure), QRS interval, and altered myocardial contraction and relaxation as indicated by the dp/dt. The administration of VKR treatment for 16 weeks effectively prevented the changes in these variables.

Hyperglycemia induces an excessive generation of reactive oxygen species by the mitochondrial electron transport chain and aggravates the formation of advanced glycation end products (AGEs)[44]. Oxidative stress plays a crucial role in the pathophysiology of DCM by promoting hypertrophy and structural damage to the cardiac tissue of individuals with diabetic condition [45]. In the present study, a decline in the levels of SOD, catalase, and reduced glutathione was observed in the cardiac tissue of diabetic rats, accompanied by an elevation in lipid peroxidation. However, these detrimental effects were ameliorated following VKR treatment signifying its antioxidant activity. Histopathological analysis revealed augmented collagen accumulation, deteriorative lesions, and fibrosis in the cardiac tissues of rats with diabetes. Administration of VKR at both dosage levels substantially protected the architecture of the cardiac tissue, leading to diminished collagen deposition and fibrosis.

The signal transduction pathway of PI3K plays a crucial role in the cellular cascade of insulin signaling. This pathway primarily induces metabolic responses, which then initiate the Akt signaling pathway. The activation of Akt leads to an increase in glucose uptake in the cardiac muscle by promoting the translocation of GLUT4 to the cell membrane of cardiac cells. Previous studies conducted in vitro and in vivo using taurine have demonstrated the downregulation of PI3K/Akt/GLUT4 in HepG2 cells and diabetic rats [46]. Similarly, a study employing carvacrol has shown significant restoration of PI3K/Akt signaling and promotion of GLUT4 membrane translocation, which was impaired in mice with T1DM and T2DM [47]. The present data indicates that VKR administration results into the activation of the PI3K/Akt/GLUT4 pathway in T2DM rats which shows VKR's beneficial role in diabetic cardiomyopathy.

The present work examined the effect of VKR in cardiomyopathy. VKR showed a well-controlled glycemic profile, potentially stemming from the effective utilization of glucose. This was additionally supported by the significant improvement in cardiac performance and biochemical parameters, coupled with reduced harm to the myocardium as indicated in histopathological findings. Moreover, the myocardial tissue exhibited better expression of PI3K/Akt/GLUT4 proteins, implying the advantageous impact of VKR on cardiovascular well-being. These findings demonstrate that VKR has a potential effect DCM. However, the study has few limitations as well. Some parameters such as 2D echo analysis of rats and estimation of fibrosis markers in cardiac tissue could have been explored. The study focused on PI3k/Akt/GLUT4 pathway and other molecular signaling pathways that have been reported for their potential role can also be studied in future to understand the detailed mechanism of VKR in DCM.

Conclusion

The present study data supports the proof that VKR has beneficial role in the management of cardiomyopathy in type 2 diabetic rats. We studied expression of PI3k, Akt, and GLUT4 by western blot; however, we could not perform RT-PCR analysis to report mRNA expressions which can be considered as limitation of the study.

Supplementary Information The online version contains supplementary material available at https://doi.org/10.1007/s12012-024-09891-0.

Author Contributions The study conception, design, and protocol were finalized by YAK and MBC. Experimentation, data collection, and analysis were performed by YAK and ADS. The first draft of the manuscript was written by ADS and all authors revised, commented, and approved the final manuscript.

Funding This study was supported by Shree Dhootapapeshwar Limited, Mumbai (India).

Data Availability The data of the study will be made available upon reasonable request to the corresponding author.

Declarations

Competing interests Mukesh B. Chawda is working with Shree Dhootapapeshwar Limited, which has funded the study. The first and corresponding author declare no conflict of interest.

Ethical Approval All experiments and procedures involving animals were approved by the SVKM's Institutional Animal Ethics Committee, protocol no. (CPCSEA/IAEC/P-14/2022).

References

1. Artasensi, A., Pedretti, A., Vistoli, G., & Fumagalli, L. (2020). Type 2 diabetes mellitus: A review of multi-target drugs. *Molecules, 25*(8), 1–20. https://doi.org/10.3390/molecules25081987
2. Pan, K. L., Hsu, Y. C., Chang, S. T., Chung, C. M., & Lin, C. L. (2023). The role of cardiac fibrosis in diabetic cardiomyopathy: From pathophysiology to clinical diagnostic tools. *International Journal of Molecular Sciences, 24*(10), 8604. https://doi.org/10.3390/ijms24108604
3. Paolillo, S., Marsico, F., Prastaro, M., Renga, F., Esposito, L., De Martino, F., Di Napoli, P., Esposito, I., Ambrosio, A., Ianniruberto, M., Mennella, R., Paolillo, R., & Gargiulo, P. (2019). Diabetic cardiomyopathy: Definition, diagnosis, and therapeutic implications. *Heart Failure Clinics, 15*(3), 341–347. https://doi.org/10.1016/j.hfc.2019.02.003
4. Kannel, W. B., Hjortland, M., & Castelli, W. P. (1974). Role of diabetes in congestive heart failure: The Framingham study. *The American Journal of Cardiology, 34*(1), 29–34. https://doi.org/10.1016/0002-9149(74)90089-7
5. Einarson, T. R., Acs, A., Ludwig, C., & Panton, U. H. (2018). Prevalence of cardiovascular disease in type 2 diabetes: A systematic literature review of scientific evidence from across the world in 2007–2017. *Cardiovascular Diabetology, 17*(1), 1–19. https://doi.org/10.1186/s12933-018-0728-6
6. Nakamura, K., Miyoshi, T., Yoshida, M., Akagi, S., Saito, Y., Ejiri, K., Matsuo, N., Ichikawa, K., Iwasaki, K., Naito, T., Namba, Y., Yoshida, M., Sugiyama, H., & Ito, H. (2022). Pathophysiology and treatment of diabetic cardiomyopathy and heart failure in patients with diabetes mellitus. *International Journal of Molecular Sciences, 23*(7), 3587. https://doi.org/10.3390/ijms23073587
7. Ke, J., Pan, J., Lin, H., & Gu, J. (2023). Diabetic cardiomyopathy: A brief summary on lipid toxicity. *ESC Heart Failure, 10*(2), 776–790. https://doi.org/10.1002/ehf2.14224
8. Ramesh, P., Yeo, J. L., Brady, E. M., & McCann, G. P. (2022). Role of inflammation in diabetic cardiomyopathy. *Therapeutic Advances in Endocrinology Metabolism, 13*, 1–13. https://doi.org/10.1177/20420188221083530
9. Aerni-Flessner, L., Abi-Jaoude, M., Koenig, A., Payne, M., & Hruz, P. W. (2012). GLUT4, GLUT1, and GLUT8 are the dominant GLUT transcripts expressed in the murine left ventricle. *Cardiovascular Diabetology, 11*, 1–10. https://doi.org/10.1186/1475-2840-11-63
10. Montessuit, C., & Lerch, R. (2013). Regulation and dysregulation of glucose transport in cardiomyocytes. *Biochimica et Biophysica Acta—Molecular Cell Research, 1833*(4), 848–856. https://doi.org/10.1016/j.bbamcr.2012.08.009
11. Jia, G., Hill, M. A., & Sowers, J. R. (2018). Diabetic cardiomyopathy: An update of mechanisms contributing to this clinical entity. *Circulation Research, 122*(4), 624–638. https://doi.org/10.1161/CIRCRESAHA.117.311586
12. Huang, X., Liu, G., Guo, J., & Su, Z. Q. (2018). The PI3K/AKT pathway in obesity and type 2 diabetes. *International Journal of Biological Sciences, 14*(11), 1483–1496. https://doi.org/10.7150/ijbs.27173
13. El-Ashmawy, N. E., Khedr, E. G., Alfeky, N. H., & Ibrahim, A. O. (2022). Upregulation of GLUT4 and PI3K, and downregulation of GSK3 mediate the anti-hyperglycemic effects of proanthocyanidins. *Medicine International, 2*(3), 14.
14. Ghafouri-Fard, S., Khanbabapour Sasi, A., Hussen, B. M., Shoorei, H., Siddiq, A., Taheri, M., & Ayatollahi, S. A. (2022). Interplay between PI3K/AKT pathway and heart disorders. *Molecular Biology Reports, 49*(10), 9767–9781. https://doi.org/10.1007/s11033-022-07468-0
15. Jaiswal, Y. S., & Williams, L. L. (2017). A glimpse of Ayurveda—The forgotten history and principles of Indian traditional medicine. *Journal of Traditional and Complementary Medicine, 7*(1), 50–53. https://doi.org/10.1016/j.jtcme.2016.02.002
16. Shah, S. (1999). *Bharat Bhaishajya Ratnakar*. B. Jain Publishers Pvt.
17. GOI, M. (2003). *Ayurvedic Formulary of India* (Vol. Part1, 2nd).
18. Gaidhani, S. N., Ala, S., Reddy, V., SanjayaKumar, Y. R., Jamadagni, S., Selvam, T., & Ajeesh Kumar, K. K. (2023). Antidiabetic activity of Vasant Kusumakar Ras in streptozotocin and high fat diet induced type 2 diabetes mellitus in Sprague Dawley rats. *Journal of Natural Remedies, 23*(2), 521–536. https://doi.org/10.18311/jnr/2023/32054
19. Tamoli, S. M., Kohli, K. R., Kaikini, A. A., Muke, S. A., Shaikh, A. A., & Sathaye, S. (2020). Vasant Kusmakar Ras, an ayurvedic herbo-mineral formulation prevents the development of diabetic retinopathy in rats. *Journal of Ayurveda and Integrative Medicine, 11*(3), 270–276. https://doi.org/10.1016/j.jaim.2020.02.002
20. Mahajan, U. B., Patil, P. D., Chandrayan, G., Patil, C. R., Agrawal, Y. O., Ojha, S., & Goyal, S. N. (2018). Eplerenone pretreatment protects the myocardium against ischaemia/reperfusion injury through the phosphatidylinositol 3-kinase/Akt-dependent pathway in diabetic rats. *Molecular and Cellular Biochemistry, 446*(1–2), 91–103. https://doi.org/10.1007/s11010-018-3276-1
21. Wang, W. Y., Twu, C. W., Liu, Y. C., Lin, H. H., Chen, C. J., & Lin, J. C. (2019). Fibronectin promotes nasopharyngeal cancer

cell motility and proliferation. *Biomedicine and Pharmacotherapy, 109*, 1772–1784. https://doi.org/10.1016/j.biopha.2018.11.055
22. Zou, Z., Dong, Y. S., Liu, D. D., Li, G., Hao, G. Z., Gao, X., Pan, P. Y., & Liang, G. B. (2021). MAP4K4 induces early blood-brain barrier damage in a murine subarachnoid hemorrhage model. *Neural Regeneration Research, 16*(2), 325–332. https://doi.org/10.4103/1673-5374.290904
23. Yin, Z., Zhao, Y., He, M., Li, H., Fan, J., Nie, X., & Wang, D. W. (2019). MiR-30c/PGC-1β protects against diabetic cardiomyopathy via PPARα. *Cardiovascular Diabetology, 18*(1), 1–15. https://doi.org/10.1186/s12933-019-0811-7
24. Srinivasan, K., Viswanad, B., Asrat, L., Kaul, C. L., & Ramarao, P. (2005). Combination of high-fat diet-fed and low-dose streptozotocin-treated rat : A model for type 2 diabetes and pharmacological screening. *Pharmacological Research, 52*, 313–320. https://doi.org/10.1016/j.phrs.2005.05.004
25. Oza, M., & Kulkarni, Y. (2020). Formononetin alleviates diabetic cardiomyopathy by inhibiting oxidative stress and upregulating SIRT1 in rats. *Asian Pacific Journal of Tropical Biomedicine, 10*(6), 254–262. https://doi.org/10.4103/2221-1691.283939
26. Tang, D., Liu, L., Ajiakber, D., Ye, J., Xu, J., Xin, X., & Aisa, H. A. (2018). Anti-diabetic effect of Punica granatum flower polyphenols extract in type 2 diabetic rats: Activation of Akt/GSK-3β and inhibition of IRE1α-XBP1 pathways. *Frontiers in Endocrinology, 9*, 1–11. https://doi.org/10.3389/fendo.2018.00586
27. Chao, P., Li, Y., Chang, C., Ping, J., & Cheng, J. (2018). Biomedicine & pharmacotherapy Investigation of insulin resistance in the popularly used four rat models of type-2 diabetes. *Biomedicine & Pharmacotherapy, 101*, 155–161. https://doi.org/10.1016/j.biopha.2018.02.084
28. Mahajan, U. B., Chandrayan, G., Patil, C. R., Arya, D. S., Suchal, K., Agrawal, Y. O., & Goyal, S. N. (2017). The protective effect of apigenin on myocardial injury in diabetic rats mediating activation of the PPAR-γ pathway. *International Journal of Molecular Sciences*. https://doi.org/10.3390/ijms18040756
29. Ohkawa, H., Ohishi, N., & Yagi, K. (1979). Assay for lipid peroxides in animal tissues by thiobarbituric acid reaction. *Analytical Biochemistry, 95*(2), 351–358. https://doi.org/10.1016/0003-2697(79)90738-3
30. Paoletti, F., Aldinucci, D., Mocali, A., & Caparrini, A. (1986). A sensitive spectrophotometric method for the determination of superoxide dismutase activity in tissue extracts. *Analytical Biochemistry, 154*(2), 536–541. https://doi.org/10.1016/0003-2697(86)90026-6
31. Johansson, L. H., & Håkan Borg, L. A. (1988). A spectrophotometric method for determination of catalase activity in small tissue samples. *Analytical Biochemistry, 174*(1), 331–336. https://doi.org/10.1016/0003-2697(88)90554-4
32. Rahman, I., Kode, A., & Biswas, S. K. (2007). Assay for quantitative determination of glutathione and glutathione disulfide levels using enzymatic recycling method. *Nature Protocols, 1*(6), 3159–3165. https://doi.org/10.1038/nprot.2006.378
33. Andonova, M., Dzhelebov, P., Trifonova, K., Yonkova, P., Kostadinov, N., Nancheva, K., & Chernev, C. (2023). Metabolic markers associated with progression of type 2 diabetes induced by high-fat diet and single low dose streptozotocin in rats. *Veterinary Sciences, 10*(7), 431. https://doi.org/10.3390/vetsci10070431
34. Mohan, M., Dihoum, A., Mordi, I. R., Choy, A.-M., Rena, G., & Lang, C. C. (2021). Left ventricular hypertrophy in diabetic cardiomyopathy: A target for intervention. *Frontiers in Cardiovascular Medicine, 8*, 1–11. https://doi.org/10.3389/fcvm.2021.746382
35. Da Dalt, L., Cabodevilla, A. G., Goldberg, I. J., & Norata, G. D. (2023). Cardiac lipid metabolism, mitochondrial function, and heart failure. *Cardiovascular Research, 119*(10), 1905–1914. https://doi.org/10.1093/cvr/cvad100
36. McNeill, J. H. (1996). Role of elevated lipids in diabetic cardiomyopathy. *Diabetes Research and Clinical Practice*. https://doi.org/10.1016/0168-8227(96)01232-6
37. Al-Rasheed, N. M., Al-Rasheed, N. M., Hasan, I. H., Al-Amin, M. A., Al-Ajmi, H. N., Mohamad, R. A., & Mahmoud, A. M. (2017). Simvastatin ameliorates diabetic cardiomyopathy by attenuating oxidative stress and inflammation in rats. *Oxidative Medicine and Cellular Longevity, 2017*, 13. https://doi.org/10.1155/2017/1092015
38. Salau, V. F., Erukainure, O. L., Olofinsan, K. A., Msomi, N. Z., Ijomone, O. K., & Islam, M. S. (2023). Ferulic acid mitigates diabetic cardiomyopathy via modulation of metabolic abnormalities in cardiac tissues of diabetic rats. *Fundamental and Clinical Pharmacology, 37*(1), 44–59. https://doi.org/10.1111/fcp.12819
39. Abukhalil, M. H., Althunibat, O. Y., Aladaileh, S. H., Al-Amarat, W., Obeidat, H. M., Alayn'Al-marddyah, A., Hussein, O. E., Alfwuaires, M. A., Algefare, A. I., Alanazi, K. M., & Al-Swailmi, F. K. (2021). Galangin attenuates diabetic cardiomyopathy through modulating oxidative stress, inflammation and apoptosis in rats. *Biomedicine & Pharmacotherapy, 138*, 111410.
40. Kaur, N., Guan, Y., Raja, R., Ruiz-Velasco, A., & Liu, W. (2021). Mechanisms and therapeutic prospects of diabetic cardiomyopathy through the inflammatory response. *Frontiers in Physiology, 12*, 1–11. https://doi.org/10.3389/fphys.2021.694864
41. Ramesh, P., Yeo, J. L., Brady, E. M., & M. G. (2022). Role of inflammation in diabetic cardiomyopathy. *Ther Adv Endocrinol Metab, 15*(13), 20420188221083530 0.
42. Fairweather, D. (2007). Regulating Inflammation in the Heart. *International Journal of Biological Sciences, 3*(1), 9–13.
43. Badole, S. L., Chaudhari, S. M., Jangam, G. B., Kandhare, A. D., & Bodhankar, S. L. (2015). Cardioprotective activity of pongamia pinnata in streptozotocin-nicotinamide induced diabetic rats. *BioMed Research International*. https://doi.org/10.1155/2015/403291
44. De Geest, B., & Mishra, M. (2022). Role of oxidative stress in diabetic cardiomyopathy. *Antioxidants*. https://doi.org/10.3390/antiox11040784
45. Liu, Q., Wang, S., & Cai, L. (2014). Diabetic cardiomyopathy and its mechanisms: Role of oxidative stress and damage. *Journal of Diabetes Investigation, 5*(6), 623–634. https://doi.org/10.1111/jdi.12250
46. Chen, B., Abaydula, Y., Li, D., Tan, H., & Ma, X. (2021). Taurine ameliorates oxidative stress by regulating PI3K/Akt/GLUT4 pathway in HepG2 cells and diabetic rats. *Journal of Functional Foods, 85*, 104629. https://doi.org/10.1016/j.jff.2021.104629
47. Hou, N., Mai, Y., Qiu, X., Yuan, W., Li, Y., Luo, C., & Luo, J. D. (2019). Carvacrol attenuates diabetic cardiomyopathy by modulating the PI3K/Akt/GLUT4 pathway in diabetic mice. *Frontiers in Pharmacology, 10*, 1–15. https://doi.org/10.3389/fphar.2019.00998